

The Impact of Dredging on Residence Time in the Amba Estuary, West Coast of India

Velamala Simhadri Naidu . Jubin Thomas . Sanjay Bari . Shubhangi Kachave

National Institute of Oceanography, Regional Centre, Lokhandwala Road, 4 Bungalows, Andheri (W), Mumbai -400053, India.

Abstract

In this study, residence time (RT) and flushing characteristics of the Amba estuary were estimated using a 2D depth-averaged model driven by hydrodynamics resulting from the bathymetry changes due to dredging carried out for ease of navigation. The model was calibrated and verified using observed data for the estuary and the model results of tides, currents and Lagrangian paths are in good agreement with the field observations. The spatial variability of RT evaluated by releasing 93 particles in the model domain during low water and high water slacks of spring and neap for the pre- and the post-dredging scenarios in dry and wet seasons indicates very high RTs in the mouth segment during flood due to the transport of particles in the eastern shallow regions. The lower neap RTs, as compared to spring during wet season, are due to the resultant seaward transport of particles facilitated by the freshwater discharge against weak neap currents. With meager dry season river discharge the trend is reversed with high neap RTs as compared to spring. Average RTs in the Amba estuary has decreased marginally by 0.2 days after dredging. The spatial variations show that the RTs are decreased in a larger area in the post dredging period except at central parts of open boundary and at mouths of Patalanganga estuary and Karanja creeks. Flushing time (FT) calculations for monsoon season show slight increase from 1.2 to 1.3 tidal cycles after dredging.

Keywords: Residence time. flushing time. modeling. lagrangian particle track. Amba estuary: India.

1. Introduction

The rate of water exchange between an estuary and the open sea plays an important role in controlling the chemical and biological processes such as planktonic biomass as well as distribution of contaminants entering these semi-enclosed bodies (Andréfouët et al. 2006; Deleersnijder et al. 1997; Lucas. 2010; Lucas et al. 2009; Monsen et al. 2002). For example, Delesalle and Sournia (1992) established a direct linear relationship between phytoplankton biomass in coral lagoons and the Residence time (RT).

The rate of exchange is generally determined by 3 time scales, viz, Flushing time (FT), age, and RT (Monsen et al. 2002). The FT is defined as ratio of the mass of a scalar in a reservoir to the rate of renewal of the scalar (Geyer et al. 2000). The FT is estimated by two approaches, viz, classical approach of tidal prism and freshwater fraction method. The tidal prism method is a relatively rough estimation of the FT as compared with the freshwater fraction method. In the freshwater fraction method, the FT is estimated using salinity and freshwater inflow (Sheldon and Alber 2002). The age is the time spent in the system by the water parcel, which enters from the boundary, before leaving from the boundary (Zimmerman 1988).

For the RT, the “timer stops” as soon as the water parcel leaves the estuary for the first time, while the other definition of the RT, known as “exposure time”, is the total time spent in the estuary as the water parcel leaves and re-enters the control domain (Bolin and Rodhe 1973; Delhez and Deleersnijder 2006; Monsen et al. 2002; Takeoka 1984; Zimmerman 1976) . Hence, the RT is dependent on the location within the estuary and tidal phase of release of a particle (van de Kreeke 1983 and Zimmerman 1988). The RT is such an important attribute that it can be the basis for comparative analyses of ecosystem-scale nutrient budgets (Boynton et al. 1995) and to assess the rate of the removal of the contaminant entering the water body (Liu et al. 2008). In the Chesapeake Bay, the RT of more than one month exacerbated eutrophication and hypoxia/anoxia due to the built-up of anthropogenic nutrients entering the estuary (Cercó and Cole 1993). Howarth et al. (2000) attributed increase in the primary production rates in the Hudson River to the increased RTs. Based on the RTs for the Musa estuary (Persian Gulf), Payandeh, Zaker and Niksokhan (2014) showed that the persistency of currents was a useful indicator for identifying areas of pollutant load accumulation. The RTs have also been studied by several authors (e.g. Luff and Pohlman 1996; Kitheka 1997; Dong and Su 1999a,b; Delhez et al. 2004; Wang et al. 2004; Fukumoto and Kobayashi 2005; Andrea and

Georg 2006; Rupali et al. 2012) mainly utilizing the concept of freshwater fraction method. The study of Brooks et al. (1999) for the Cobscook Bay (Maine) using the Lagrangian particle track method demonstrated significant contribution (>50%) of the tidal transport to flushing when the river discharge was below its long-term mean.

Among other factors, the tidal propagation in an estuary is a function of its bathymetric configuration which in turn is influenced by natural processes and human-induced changes. Thus, accretion in the mouth segment which is common and sometimes seasonal, in many estuaries leads to tidal energy losses creating flood dominance. Anthropogenic interventions such as reclamation, construction of harbours, flood control measures etc often result in an increase in the RT due to decreased estuarine volume. On the other hand, the dredging in the estuary – often to enhance navigation at the inlet regions leads to positive effects by facilitating increase in volume of seawater entering the system. Gong et al. (2008) have shown that the average RT of the Xiaohai Lagoon had increased from 45 to 71 days due to human-induced changes in the upstream. On the other hand, the average RT of the O´bidos lagoon significantly decreased from 1 year to 6 months due to the channel made at the throat of the inlet (Oliveira et al. 2006). The general perception is that the RTs are smaller during larger tidal prism (spring) and higher in the neap. However, Olivera and Baptista (1997) found relatively larger RTs when the particle was released at spring high water slack. Vijit et al. (2009) estimated the FT and studied freshwater influence on the salinity distribution of the Mandovi estuary, India. They found that the entire estuary will become river during the monsoon due to salinity egress. In contrast, ingress is felt upto upstream in dry season making the estuary unsteady. Based on the particle track method, Rupali et al. 2012 studied the RT of the bio-rich Gulf of Kachchh, India, which occupies an area of 7300 km² and receives effluents from several sources, and found that RT of the Gulf was relatively small thereby promoting efficient removal of contaminants from the water body. Dinesh Kumar and Sarma. 1991 estimated the FT of the Amba estuary based on the application of the tidal prism method and found that it varied between 1.3 to 1.7 tide cycles for freshwater discharge rate of 96 m³ s⁻¹ which increased to 2.2 - 4.6 tide cycles as the summer approached and the river freshwater inflow decreased to 9.6 m³ s⁻¹. However, the effect of dredging on the RT of a monsoonal estuary has not been studied.

In this study, an attempt has been made to study the effect of dredging on the RT of the Amba estuary using Lagrangian particle track method in a 2D numerical model. The model was calibrated with

observed tides and currents and verified with the observations of Lagrangian paths. The calibrated model was applied to estimate the spatial variability of RTs of the Amba estuary by releasing particles at different locations at different tidal phases in monsoonal freshwater discharge and dry conditions representing before and after dredging scenarios. Flushing characteristics of the estuary were also studied using tidal prism method.

2. Study Region

The Amba River, which originates in the Western Ghats of the Indian subcontinent, follows a narrow and meandering course along her length of over 140 km before opening into the Mumbai Harbour (Fig. 1). Along the estuary, small towns like Rewas, Dharmatar, Kharjui and Nagothane are situated. Two tidal inlets of the Patalaganga estuary and Karanja Creek join the Amba in the lower reaches before its confluence with the Mumbai Harbour. A dam, constructed across the river at Nagothane (about 50 km upstream from the mouth), impounds the riverine flow, forming the source of supply of freshwater through the water supply scheme of the Maharashtra Industrial Development Corporation (MIDC). The dam gates are generally kept open during the monsoon (June to September), allowing the riverine flow into the tidal waters. The freshwater discharge through the dam is restricted after September and is considered negligible during the non-monsoonal months. The lower reaches of the estuary is navigable up to the Dharamtar jetty.

Annual rainfall averages around 2100 mm with 95% precipitation occurring during the monsoon months. Winds are southwesterly during monsoon with speeds ranging from 2 to 20 km h⁻¹ but barely exceed 12 km h⁻¹ over the dry season with the change in direction to northeasterly. Due to funnel effect, the tide increases upto Dharmatar and decreases in the upstream upto Nagothane. The peak discharge during monsoon peaking at 550 m³ s⁻¹ promotes continuous ebb upto Kharjui. The salinity which is comparable to that of fresh water at Nagothane during monsoon remains low (0-5) upto Dharamtar with a marked increase in the downstream and values exceed 30 in the mouth segment. With the withdrawal of monsoon the salinity rises sharply with values around 27 at Nagothane and often exceeds 36 at the mouth. The estuary is shallow with the depth of 6 m at the mouth decreasing to barely 2 m at Nagothane.

Establishment of few industries, namely Maharashtra Gas Cracker Complex (MGCC), Supreme Petrochemicals Limited and Ispat Industries Limited, along the Amba estuary has catalyzed the

development of the area leading to enhanced human settlements as well as commercial and infrastructural facilities. The MGCC discharges its petrochemical effluents to the tune of 6500 m³ d⁻¹ at a site between Dharamtar and Mankhule. After the Jetty at Dharamtar was made operational in 1995, Maharashtra Maritime Board (MMB) has been maintaining a channel with depth of 3.5 m below spring low water and width of 135 m from the mouth to Dharamtar for navigation of barges. About 13 chemical industries established in the MIDC area adjacent to the Patalaganga estuary release their combined effluent of 10000 m³ d⁻¹ which is ultimately transported to the Amba. The Amba-Patalganga estuarine complex has extensive mangrove formations which are classified as ecologically sensitive. Their ecology however has not attracted much attention.

3. Model

Since the Amba estuary is shallow with well mixed water column, an unsteady, two-dimensional vertically integrated shallow-water equation for continuity and momentum balance given by Stoker (1957) has been used to obtain the tides and tide-induced circulation in the estuary. **In this study, a 2D model developed for simulating Thane creek tidal circulation has been applied to the estuary (Naidu and Sarma, 2001).** The coriolis parameter was taken as $4.75 \times 10^{-5} \text{ s}^{-1}$. The bottom friction (C_f) was parameterized in terms of coefficient of Chezy using the formula, $C_f = (1/32) \times [\log_{10} (14.8 H)/K]^2$. Where K is a roughness length and H is the total depth. Stability of the numerical scheme is governed by $\Delta t < \Delta x / \sqrt{2gH_{max}}$. Where Δx is grid size in meters and Δt is the time step in seconds and g is the acceleration due to gravity and H_{max} is the maximum depth in the model domain. As H_{Max} is 6 m and Δx is 100 m, the Δt may be 9 s. It was assumed that initially the sea is at rest, ie, at $t=0$, horizontal velocity components (U&V) = 0. The Rewas tide data was specified as the boundary condition in the west. The southern boundary was closed during non-monsoon season and opened during the monsoon season.

Lagrangian particle track was calculated using the equation (Gong et al. 2008)

$$\bar{x}(t + \Delta t) = \bar{x}(t) + \bar{U} * \Delta t + z_n \sqrt{2 * d_h * \Delta t} \quad 1$$

where \bar{x} is the particle's position, Δt = time step, d_h = horizontal diffusion coefficient and z_n = random vector. In this work, diffusion term is neglected.

We estimated FT using the tidal prism model as reported by Sheldon and Alber (2002).

$$T_f = V_h/V_{tp} \quad 2$$

Where T_f is the FT, V_h is estuary volume at high tide (Luketina. 1998), V_{tp} is the tidal prism or the volume that entered during low water and high water. In the above equation, freshwater influence is not taken into account. The formula suggested by Luketina (1998) was used in the study.

$$V_{tp} = Q_{FW} + Q_{FL} \quad 3$$

Where Q_{FW} is freshwater inflow during tidal period and Q_{FL} is the volume of seawater entering into the estuary during flood tide.

The 2 sets of bathymetry maps drawn out of the data collected in 1985 and 2000 representing pre-dredging and post-dredging scenarios were digitized and are shown in figure. 2. The mouth region of the Amba estuary is shallow with the depths of 6 m below chart datum which is defined as the lowest low water level. Tide data of Dharamtar recorded in 1986 and 2007 indicate that tide is mixed semi-diurnal with two unequal amplitudes with the maximum spring tide of 5.1 m and neap tide of 3.0 m. Field drogue study was conducted on 28 November 1986 by releasing a neutrally buoyant drogue at Dharamtar at 0930 h and its geographical location was recorded at every 30 min interval up to 1900 h. The Lagrangian path was used to calibrate the model for pre-dredging scenario. Additional tide data was collected at Dharamtar during the period 26 May 2007 to 02 June 2007 and the currents were recorded at Mankhule for the same period using Falmouth make ACM current meter. Three drogue studies conducted in the Amba estuary on 19 November 2000, 20 November 2000 and 31 May 2007 were used to verify the results for the post-dredging scenario.

3.1 Calibration

Initial condition was assumed as specified in the earlier section. Tide data at Rewas was prescribed at the western boundary and the model run started from 16 November 1986 at 1400 h to 03 December 1986 at 1853 h. The first one day output of the model was discarded as the instabilities crop up during the simulation due to cold start initial condition. The model was run by varying coefficient, K , in the bottom friction formula. The comparison of modeled tide of Dharamtar, which was stored at 15

min interval, with the observations (Fig. 3a) reveals a fair agreement between the two with correlation coefficient of 0.92. Hence, the value of K was fixed as 0.065.

3.2 Verification

The model was run for the same model domain with deeper channel from mouth to Dharamtar using the bathymetry of 2000 (Fig. 2). The tide data at Rewas was used as a boundary. The comparison of observed and modeled tide at Dharamtar (Fig. 3b) indicates that the simulations are in fair agreement with the observations with correlation coefficient (r) of 0.8. The model was run again for Lagrangian particle track by releasing a particle at Mankhule. The model run started on 27 November 1986 at 0930 h and ended on 28 November 1986 at 1900 h. The model results of the particle track were stored at 30 min intervals. A comparison made with the drogue trajectory of 28 November 1986 (Fig. 4a) indicates that the particle trajectory is elliptical in nature and excursion length of the modeled trajectory (15.1 km) is in agreement with the observation (15.1 km). Comparison of observed circulation path (5.1 km) collected during ebb to flood on 19 November 2000 with modeled track (4.9 km) indicates that deviation in the track is 0.2 km (Fig. 4b). The observed trajectory (9.9 km) of 20 November 2000 which represents flood to ebb is also compared with the modeled trajectory (10.1 km). The deviation in this case is also 0.2 km (Fig. 4c). The model was also compared with the drogue study carried out on 31 May 2007 from 0600 h to 1730 h. Figure 4d shows that the excursion length obtained from simulated lagrangian particle track (10.5 km) is nearly equivalent to the observations (10.7 km). The above verification results show the model simulates the lagrangian path with reasonable accuracy.

The currents measured at Mankhule were compared with the modeled currents (Fig. 5). The observed current speeds during ebb were erroneous as the deployed current meter made an inclined angle with vertical. Hence the comparison was made with the observations during flood only by calculating the correlation coefficient. The results are in reasonable agreement with $r = 0.75$.

4. Results and Discussion

The impact of dredging in the Amba estuary on the RT scales has been studied. Model was run for 30 days in 8 cases, viz, low and high water slacks during neap and spring for dry and wet conditions. Model was set up for 2 different bathymetric scenarios, before and after dredging. A total 93

locations were selected in the model domain to release particles. In each run, the particle trajectory computation stops when it reaches the boundary.

4.1 Before dredging

The model was run to calculate current vectors for before dredging condition (Fig. 6). Maximum current velocity of 1.05 m s^{-1} (1.6 m s^{-1}) is found during spring ebb (flood) at the place between Dharamtar and Mankhule. Ideally the RTs are measured by releasing particles at a location in each water grid cell at different tidal phases. Average monsoonal discharge was considered as suggested by Dinesh Kumar and Sarma, 1991. Since the river runoff of the Patalaganga estuary is not available, 20% of the Amba estuary's runoff is assumed for wet season. The model was run for dry season without giving freshwater discharge at the upstream covering neap and spring tide regimes. Figure 7 shows the RT distribution in the estuary for low tide slack of neap and spring during wet and dry season. Generally RTs are lower during neap as compared to spring releases in the wet season. On the contrary, during spring, tidal influence dominates the freshwater discharge resulting relatively larger RTs in the domain. In case of dry season (Fig. 7c&d), relatively low values are found at mouth region in the neap than the spring counterparts. However, in the upstream, spring RTs are lower than the neap RTs. In the absence of influx from the upstream, particle drifting is controlled by the tidal waters. In all 4 cases, a total of 68 particles do not reach the boundary and RTs of other particles range between 0.3 and 8.7 days.

Very high RTs are noticed at mouth region during spring flood releases. Why does a particle at the mouth region have more RTs than that found in the upstream region during flood? To observe the particles trajectories released at selected locations, the model was run for the above conditions and shown in the figure 8. Particle released at location #92 does not reach the boundary in all 4 cases. More particles reach the boundary during neap as compared to the spring. Particle released at location #80 enters the Patalaganga estuary. The figure clearly shows that the particles released at the boundary during flood in the spring tide reach the mud flats in the east and upstream of the Patalaganga estuary. This leads to very high RTs in this region during this period.

Now the model was run for the releases of high water slack and results are presented in figure 9. The releases during spring have lower RTs as compared to the neap in the wet season. Even though there is no much difference between spring releases during dry and wet season, the neap releases during dry

season have higher RTs. In this case also, RTs are higher in the upstream. In case of high tide releases, eastern part, opposite to the inlet mouth, has consistently high values as the region is shallow and currents are parallel to the coast.

Averages of releases – spring, neap, dry and wet - were calculated for each location. Out of the 744 releases, 87 particles do not reach the boundary in 30 days. The average values range from 0.02 days to 8.7 days for the particles reaching the boundary. Maximum RTs are found in the upstream segment of the estuary and the range is between 3.9 and 8.7 days. The region at the inlet mouth experiences RTs between <0.1 and 1.7 days. Overall average RT of the domain is 4.6 days.

To know the tidal propagation in the estuary, tidal elevation is stored at each 5 min interval at 3 locations in the estuary starting from inlet mouth. The results show that tide at the upstream (near Dharmatar) lags by 18 to 36 min depending on the tide (spring; neap) and flow condition. During wet season tidal propagation is controlled by both tide and upstream discharge. In the dry season the propagation is controlled by the tide only. The time lag is smaller (higher) during wet (dry) season. The tidal range decreases towards upstream and the range is reduced to about 0.1 m at Dharmatar.

4.2 After Dredging

The model was run for the boundary conditions that were used in 1986 scenario with modified bathymetry. The modeled current vectors representing spring ebb and flood are presented in the figure 10. The maximum current velocities during flood and ebb are 1.4 m s^{-1} and 1.2 m s^{-1} respectively. Maximum currents are found in the channel south of Mankhule.

RTs of the particles released in the low tide slack are presented in the figure 11. Out of the 93 particles 19 particles do not reach the boundary during neap tide of wet condition. The RTs range from 0.3 to 4 days. In this case also, relatively high RTs are found at mouth in spring as compared to the neap tide condition. In the upstream of the estuary, larger RTs are noticed during wet season. However, during dry season very low values (0.3 to 2.0 days) are found in this region. When it is compared with the 1986 scenario, small RTs are found during spring dry season in the upstream. Nearly 18 particles in each run did not reach the boundary, even though some of them are close to the boundary. Figure 12 indicates that RTs of spring releases in both dry and wet season are low as compared to the neap releases. Overall ebb tide releases have lower RTs than that of the flood

releases. The averages of 8 cases, low tide, high tide, neap, spring of dry and wet seasons range from <0.1 to 11.8 days. Higher RTs are found in the central basin and upstream. Lower RTs are found in the region between Mankhule and Dharamtar where dredging was carried out. The average RT in the domain is 4.4 days. Out of 744 particles released, 80 particles did not return to the boundary. In this case also, particles released at location #80 enter into the Patalaganga estuary except during wet season of spring tide (Fig. 13). Out of 36 releases, 6 particles, mostly during dry season, do not reach the boundary. The figure shows that particle advects more towards upstream during the dry season as compared to before dredging period. As a result, excursion lengths during flood have increased considerably after dredging. Tidal propagation in the estuary demonstrates that time lag between the mouth and the upstream ranges from 12 to 24 min which is lower than that obtained for pre-dredging period. This shows that the tidal propagation is increased by about 30% during flood tide after dredging.

FT was calculated by running the model for tidal elevation of spring and neap for wet season of 1986 (before dredging) and 2007 (after dredging). Volume of the estuary below low water in 1986 was $3.8 \times 10^7 \text{ m}^3$. By dredging the channel, the volume is increased to $4.3 \times 10^7 \text{ m}^3$. When peak monsoonal flow is considered, the FT before dredging was 1.2 tide cycles. After dredging it is 1.3 tide cycles. This shows that the flushing of the estuary is slightly decreased due to dredging the channel. When compared to the earlier study of Dinesh Kumar and Sarma (1991) the results are comparable. Estimation of flushing time represent for the whole estuary while RT is function of place and tidal phase. This represents the monsoon condition.

Generally it is believed that RTs of a particle released during spring low water are relatively shorter than the particle released in neap tide. Spring waters have high tidal prisms and cause rapid removal of the particle. However, in this study we find low RTs during neap tides and high RTs in spring during wet season. This study supports the results of Oliveira and Baptista (1997). During dry season, the situation is reversed as particles have more RTs during neap as compared to spring. In the absence of freshwater discharge, particle movement is restricted by tidal currents leading to low RTs during spring.

Particles released during ebb have consistently low RTs than flood releases. Relatively greater RTs are found during dry season. The particles under the influence of freshwater discharge travel rapidly towards boundary resulting in lower RTs. In general RTs are greater in the upstream region even

during monsoon also. Most of the particles released in the upstream are moving towards shallow mud flats situated along the upstream. This may be the reason for development of vast mudflats in the region.

The study of Gong et al. (2008) showed that reclamation on the banks has increased the RT. Oliveira et al. (2006) found that dredging of the channel at the inlet mouth decreased the RTs. In the former case, the reclamation in the upstream regions reduces the estuarine volume. On the other hand in the latter case, the estuarine volume is increased due to dredging leading to relatively low RTs after dredging. In the present study, dredging was carried out in the model domain starting at around 1 km from the boundary. In the present case also estuarine volume is increased due to dredging without altering tidal prism. The tidal propagation in the dredged channel is altered due to changes in the bottom frictional forces. As a result, currents in the region are strong and increase the excursion lengths in the upstream. Relatively ebb currents dominate the flood currents resulting in slightly lower RTs after dredging.

During spring, particle entered into the Patalaganga estuary mouth region which is close to the western boundary with a distance of 7 km. In the low tide, the currents are directed towards the western boundary in the downstream of the estuary. However, a particle present at the downstream in low water slack is pushed towards the Patalaganga estuary mouth during spring high water due to high currents generated by larger tidal volumes. This led to particle movement towards the Patalaganga estuary and Karanja creek.

As expected, dredging the channels increases the tidal propagation and amplitudes in the estuaries. Even though inlet mouth is not altered, the channel deepening within the estuary causes change in tidal propagation due to bottom frictional forces. In a shallow channel, tidal propagation is retarded due to high bottom friction. On the other hand, it enhances due to deeper channels. This effect leads to high excursion lengths during flood. The results of the present study suggest that the modification in the channel geometry increases tidal amplitudes by 30% after dredging and tidal phase lag between Dharamtar and inlet mouth is decreased by 6 -12 minutes. Average RT before dredging is 4.6 days and 4.4 days after dredging. A marginal decrease of 0.2 days is found in this study. The number of particles reaches the boundary is more after the dredging.

Figure 14 shows the spatial variations in anomalies of RTs due to dredging in the Amba estuary. Positive (negative) values indicate lower (higher) RTs after (before) dredging. From this figure, it is discerned that RTs in the upstream region have considerably decreased after dredging. However, RTs have increased at boundary and mouths of the Patalaganga estuary and Karanja creek. In general, RTs decrease spatially after dredging.

5. Conclusions

Generally, RTs are higher at mouth region for flood releases as the particles reach the mudflats present opposite to the boundary. The upstream of the estuary also has high RTs. During wet season, RTs are lower in neap as compared to spring due to domination of freshwater discharge in the upstream than the prevailing neap currents. Tidal propagation is increased by 30% after dredging. Particles released at mouth of the Amba river channel enter the Patalaganga estuary and Karanja creeks. FT, which is calculated for freshwater discharge, is slightly increased by 0.1 tidal cycle after dredging. Average RT decreased marginally by 0.2 days after dredging due to variation in tidal propagation and increase in estuarine volume. After dredging, low RTs are found in the larger areas except in the vicinity of the open boundary, mouths of Patalaganga estuary and Karanja creek.

The Amba estuary has salinity of nearly 35 at the mouth region and it is more or less maintained during dry season to upstream (Anonymous NIO/SP-10/2013). However, during monsoon, salinities of less than 5 are observed to the middle of the estuary. The dredging at the inlet is responsible for the increased tidal inflow to the estuary leading to increasing excursion of high saline water to the upstream. The effect of the dredging on the salinity excursion is not known. Both banks of the estuary have mangroves which are different species in terms of salinity tolerance (Kulkarni et al. 2011). Hence a study should be aimed at the impact of dredging on salinity variation in the estuary.

Acknowledgements

The authors are grateful to Dr. S. N. Gajbhiye, Scientist-in-Charge, Dr. S.W.A Naqvi, Director, National Institute of Oceanography, India, for their constant encouragement and support during the work. Authors would also like to express their gratitude to Lisa V. Lucas, Geological Survey, US for her comments on this manuscript.

References

- Andréfouët S, Ouillon S, Brinkman R, Falter J, Douillet P, Wolk F, Smith R, Garen P, Martinez E, Laurent V (2006) Review of solutions for 3d hydrodynamic modeling applied to aquaculture in south pacific atoll lagoons. *Marine Pollution Bulletin* 52 (10):1138–1155
- Andrea Cucco, Georg Umgiesser (2006) Modelling the venice Lagoon residence time. *Ecological modeling* 193:34-51
- Anonymous (2013) Periodic monitoring of Amba estuary. NIO/SP-10/2013
- Bolin B, Rodhe H (1973) A note on the concepts of age distribution and transit time in natural reservoirs. *Tellus* 25:58-62
- Boynton WR, Garber JH, Summers R, Kemp WM (1995) Inputs, transformations, and transport of nitrogen and phosphorus in Chesapeake Bay and selected tributaries. *Estuaries* 18:285–314
http://www.gonzo.cbl.umces.edu/documents/nutrients/Est18_1995.pdf
- Brooks D A, Baca MW, LoY-T (1999) Tidal circulation and residence time in a macro tidal estuary: Cobscook Bay, Maine. *Estuar Coast Shelf Sci* 49:647–665
<http://www.jstor.org/stable/60225647?seq=1>
- Cerco C, Cole T (1993) Three dimensional eutrophication model of Chesapeake Bay. *ASCE Journal of Environmental Engineering* 119 (6):1006–1025
- Deleersnijder E, Tartinville B, Rancher J (1997) A simple model of the tracer flux from the Mururoa lagoon to the Pacific. *Applied Mathematics letters* 10:13-17
- Delesalle B, Sournia A (1992) Residence time of water and phytoplankton biomass in coral reef lagoons. *Continental Shelf Research* 12 (7-8):939-949
- Delhez EJM, Deleersnijder E (2006) The boundary layer of the residence time field. *Ocean dynamics* 56:139-150
- Delhez EJM, Heemink AW, Deleersnijder E (2004) Residence time in a semi-enclosed domain from the solution of an adjoint problem. *Estuar Coast Shelf Sci* 61(4):691-702
- Dinesh Kumar PK, Sarma RV (1991) Flushing Characteristics of Amba river estuary, west coast of India. *Indian Journal of Marine Sciences* 20:212 – 215 <http://drs.nio.org/drs/handle/2264/3329>
- Dong LX, Su JL (1999a) Numerical study of the water exchange in Xiangshangang Bay. Part one: advection-diffusion tidal exchange model. *Oceanologia et Limnologia Sinica* 30:410-415 (in Chinese, with English abstract)
- Dong LX, Su JL (1999b) Numerical study of the water exchange in Xiangshangang Bay. Part two: model application and water exchange study. *Oceanologia et Limnologia Sinica* 30:465-470 (in Chinese, with English abstract)

Fukumoto T, Kobayashi N (2005) Bottom stratification and water exchange in enclosed bay with narrow entrance. *Journal of Coastal Research* 21:135-145

Geyer WR, Morris JT, Pahl FG, Jay DA (2000) Interaction between physical processes and ecosystem structure: A comparative approach, pp 177 -206. In J. E Hobbie [ed], *Estuarine science: A systematic approach to research and practice*, Island press

Gong WP, Shen J, Jia JJ (2008) The impact of human activities on the flushing properties of a semi-enclosed lagoon: Xiaohai, Hainan, China. *Marine Environmental Research* 65:62 – 76

Howarth RW, Swaney DP, Butler TJ, Marino R (2000) Climatic control on eutrophication of the Hudson river estuary. *Ecosystems* 3:210–215
ftp://ftp.ldeo.columbia.edu/pub/bnewton/HRLit/chemistry/HowarthRW_etal_Ecosystems00_Climatic_Control_Eutrophication_HRE.pdf

Kitheka JU (1997) Coastal tidally-driven circulation and the role of water exchange in the linkage between tropical coastal ecosystems. *Estuar Coast Shelf Sci* 45:177-187
<http://www.sciencedirect.com/science/article/pii/S0272771496901894>

Kulkarni VA, Naidu VS, Jagtap TG (2011) Marine ecological habitat: A case study on projected thermal power plant Dharamtar creek, India. *Journal of Environmental Biology* 32:213-219
<http://drs.nio.org/drs/handle/2264/3809>

Liu W-C, Chen, Wei-Bo, Kuo, Jan-Tai, Chin, Wu (2008) Numerical determination of residence time and age in a partially mixed estuary using three dimensional hydrodynamic model. *Continental Shelf Research* 28:1068–1088

Lucas LV (2010) Implications of the estuarine transport for water quality. In: Valle-Levinson, A. (Ed.), *Contemporary issues in estuaries physics*. Cambridge University Press, UK, pp 273-307

Lucas LV, Thompson JK, Brown, LR (2009) Why are diverse relationships observed between Phytoplankton biomass and transport time? *Limnology and Oceanography* 54:381-390

Luff R, Pohlman T (1996) Calculation of water exchange times in the ICEBoxes with an Eulerian dispersion model using a half-life time approach. *German Journal of Hydrography* 47:287-299

Lukentina D (1998) Simple tidal prism model revisited. *Estuar Coast Shelf Sci* 46:77-84

Monsen NE, Cloern JE, Lucas LV, Monismith SG (2002) Comment on the use of flushing time, residence time and age as transport time scales. *Limnology and Oceanography* 47(5):1545-1553

http://www.science.calwater.ca.gov/pdf/iep_sag/Residence_Time_Monsen_et_al.pdf

Naidu VS, Sarma RV (2001) Numerical modeling of Tide-induced currents in Thane creek, West coast of India. *Journal of Waterway, Port, Coastal and Ocean Engineering* 127(4):241-244

<http://ascelibrary.org/doi/10.1061/%28ASCE%290733-950X%282001%29127%3A4%28241%29>

Oliveira A, Baptista A M (1997) Diagnostic modeling of residence time in estuaries. *Water Resources Research* 33(8):1935–1946

Oliveira A, Fortunato AB, Rego JRL (2006) Effect of morphological changes on the hydrodynamics and flushing properties of the Obidos Lagoon (Portugal) *Continental Shelf Research* 26:917-942

http://www.academia.edu/314181/Effect_of_Morphological_Changes_on_the_Hydrodynamics_and_Flushing_Properties_of_the_Obidos_Lagoon_Portugal

Payandeh A, Zaker NH, Niksokhan MH (2014) Numerical modeling pollutant load accumulation in the Musa estuary, Persian Gulf, *Environ Earth Sci*, (in press) doi: [10.1007/s12665-014-3409-0](https://doi.org/10.1007/s12665-014-3409-0)

Rupali S, Vethamony P, Lokesh KS, Babu MT (2012) Residence time of pollutants discharged in the Gulf of Kachchh, northwestern Arabian Sea, *Marine Pollution Bulletin* 64:1659 – 1666
<http://drs.nio.org/drs/handle/2264/4141>

Sheldon JE, Alber M (2002) The calculation of estuarine turnover times using freshwater fraction and tidal prism models: a critical evaluation. *Estuaries and coasts* 29:133-146

Stoker JJ (1957) *Water waves*, Interscience Publishers, New York

Takeoka H (1984) Fundamental - concepts of exchange and transport time scales in a Coastal Sea. *Continental Shelf Research* 3:311-326

Van de Kreeke J (1983) Residence time: application to small boat basins. *ASCE Journal of Waterway, Port, Coastal and Ocean Engineering* 109 (4):416-428

Vijith V, Sundar D, Shetye SR (2009) Time-dependence of salinity in monsoonal estuaries, *Estuar Coast Shelf Sci* 85:601-608 <http://drs.nio.org/drs/handle/2264/3457>

Wang Chi-Fang, Ming-His Hsu, Albert YKuo (2004) Residence time of the Danshuei River estuary, Taiwan. *Estuar Coast Shelf Sci* 60(2004):381 -393
http://www.ae.ntu.edu.tw/files/writing_journal/9/63_baf51caa.pdf

Zimmerman J (1976) Mixing and flushing of tidal embayment in the western Dutch wadden Sea part i: distribution of salinity and calculation of mixing time scales. *Netherlands Journal of sea Research* 10(2):149-191

Zimmerman J T F (1988) Estuarine residence times. In B Kjerfve[ed.], *Hydrodynamics of estuaries 1*: CRC press

Figures:

- 1 Location map with model domain
- 2 Bathymetry map (a) before dredging (b) after dredging
- 3 Comparison of observed and predicted tide at Dharamtar (a) before dredging (b) after dredging
- 4 Comparison of observed and predicted Lagrangian path (a), (b), (c) before dredging (d) after dredging
- 5 Comparison of observed and predicted currents at Mankhule during 2007
- 6 Modeled current velocity vectors BD during (a) ebb (b) flood.
- 7 Modeled RT during flood before dredging (a) neap flow (b) spring flow (c) neap without flow (d) spring without flow.
- 8 Modeled lagrangian tracks during flood before dredging (a) neap flow (b) spring flow (c) neap without flow (d) spring without flow.
- 9 Modeled RT during ebb before dredging (a) neap flow (b) spring flow (c) neap without flow (d) spring without flow.
- 10 Modeled current velocity vectors after dredging during (a) ebb (b) flood.
- 11 Modeled RT after dredging during flood (a) neap flow (b) spring flow (c) neap without flow (d) spring without flow.
- 12 Modeled RT after dredging during ebb (a) neap flow (b) spring flow (c) neap without flow (d) spring without flow.
- 13 Modeled lagrangian tracks after dredging during flood; (a) neap flow (b) spring flow (c) neap without flow (d) spring without flow.
- 14 Anomalies in average RTs before (+ values) and after (- values) dredging scenarios

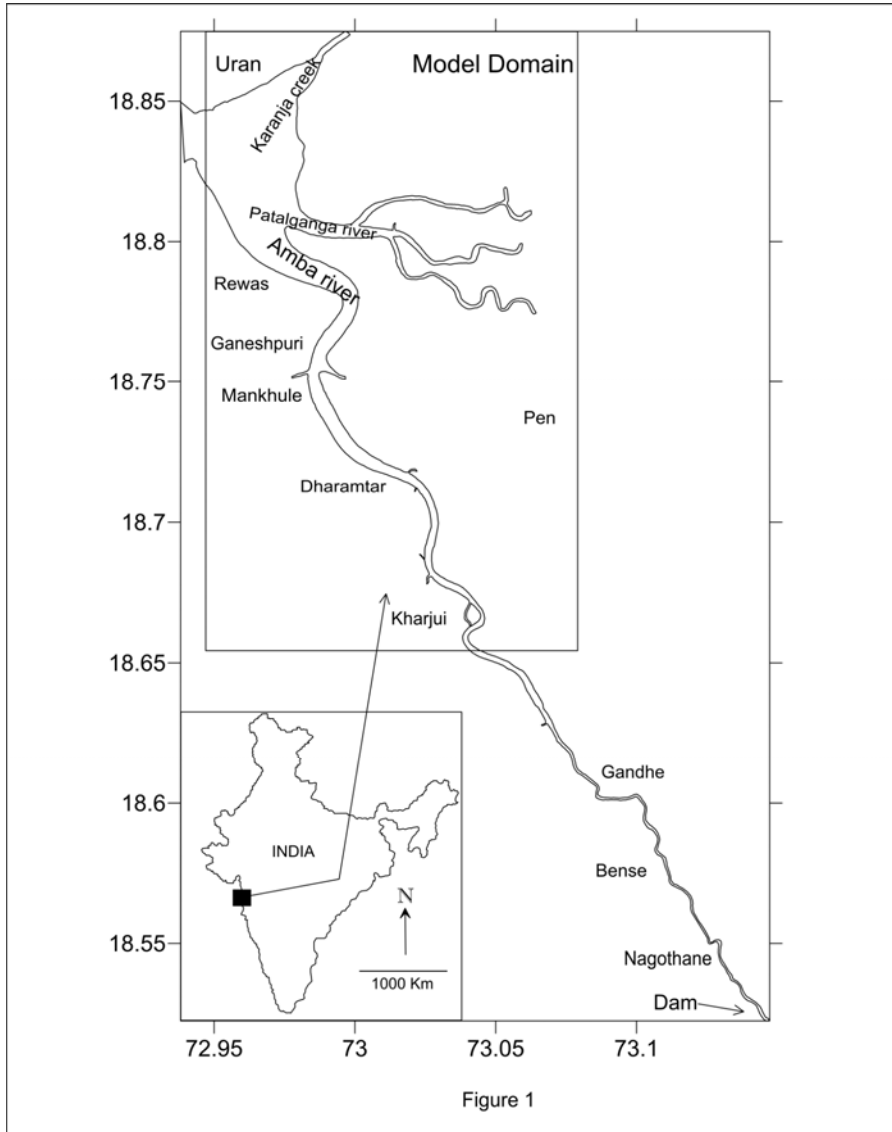


Figure 1

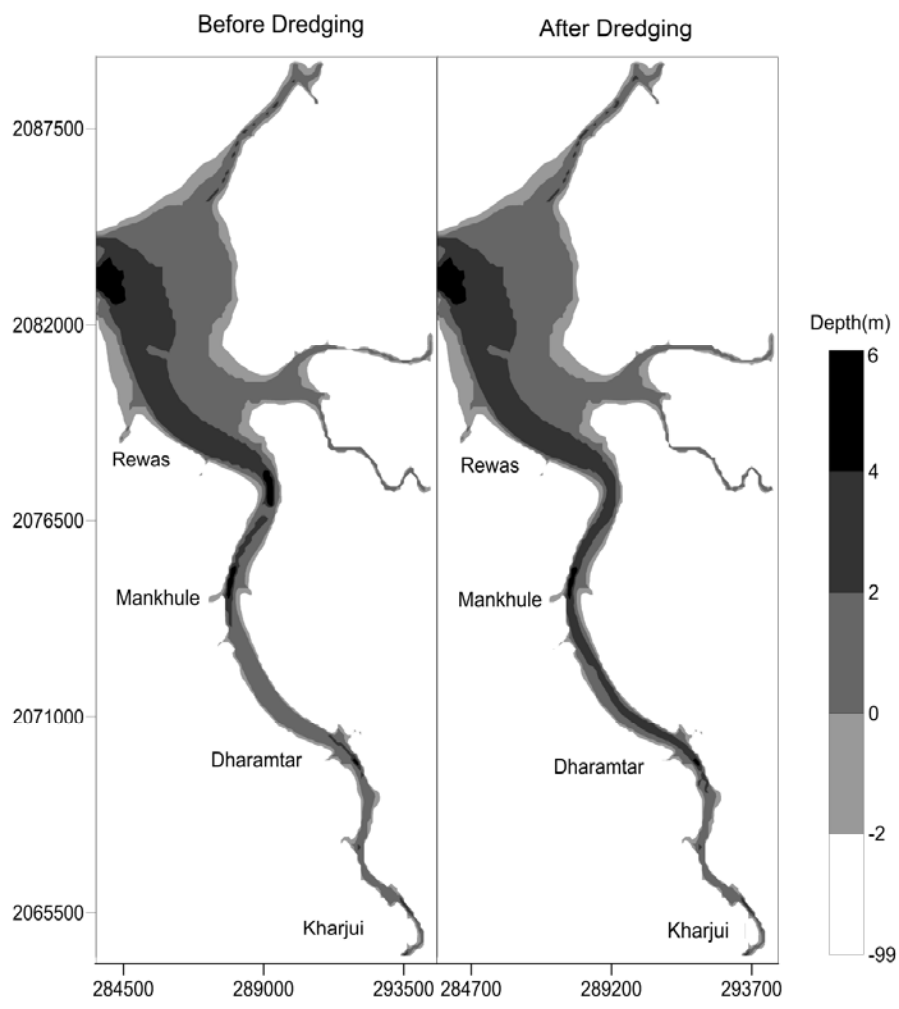


Figure 2

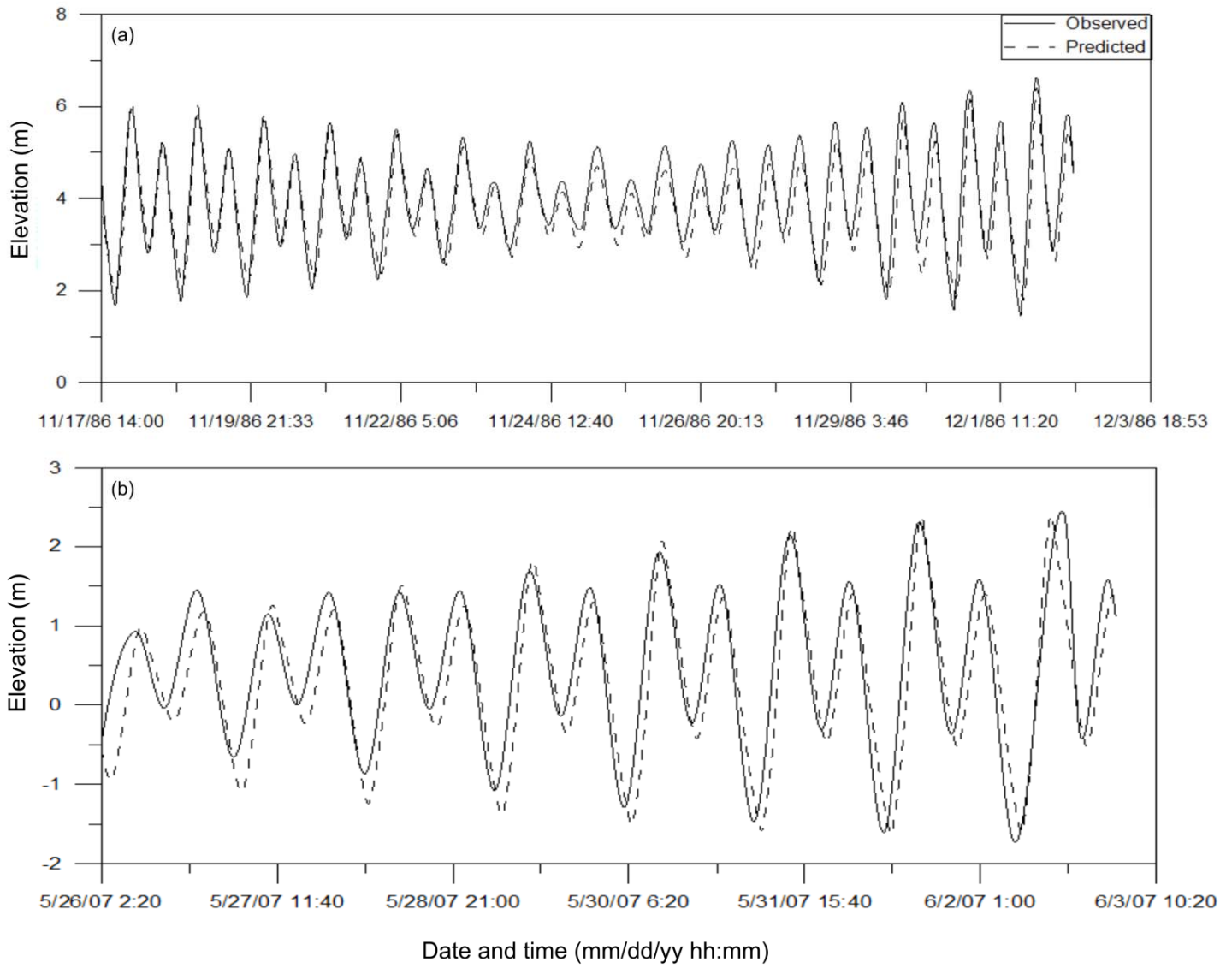


Figure 3

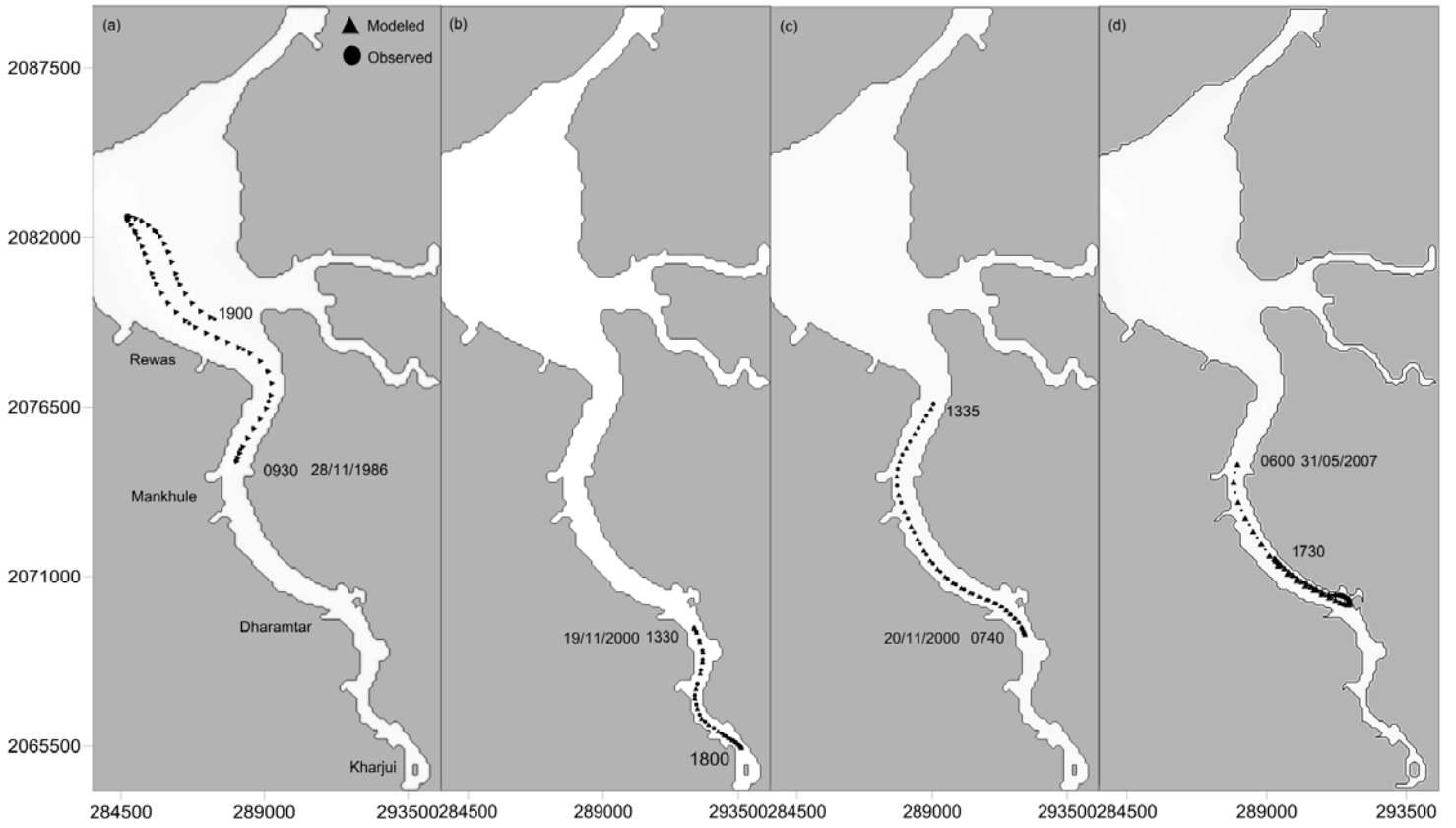


Figure 4

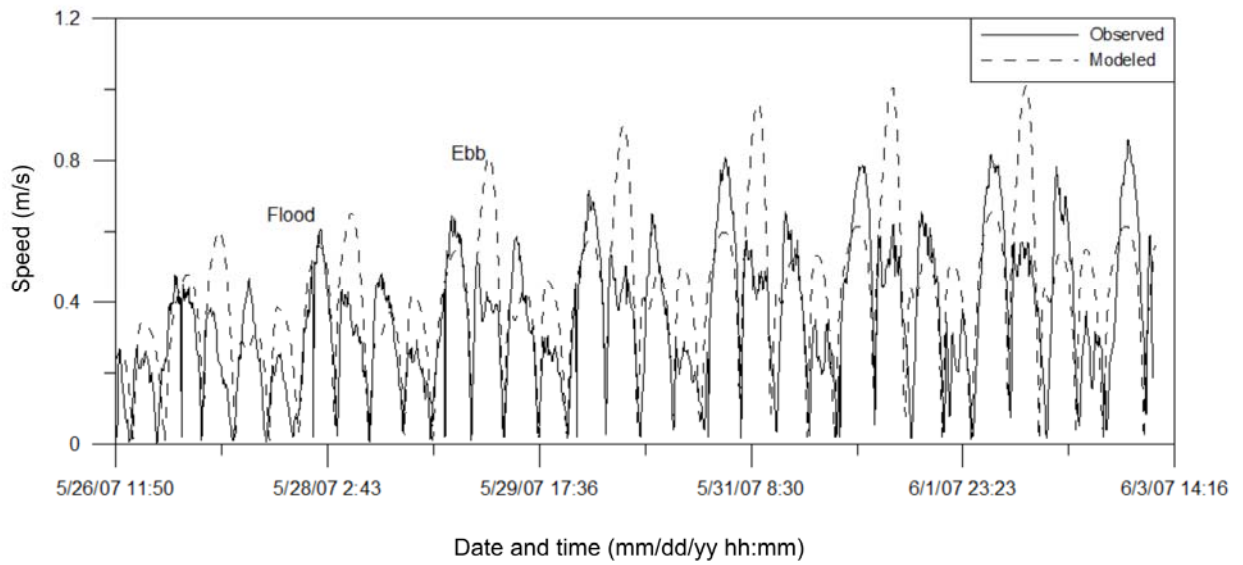


Figure 5

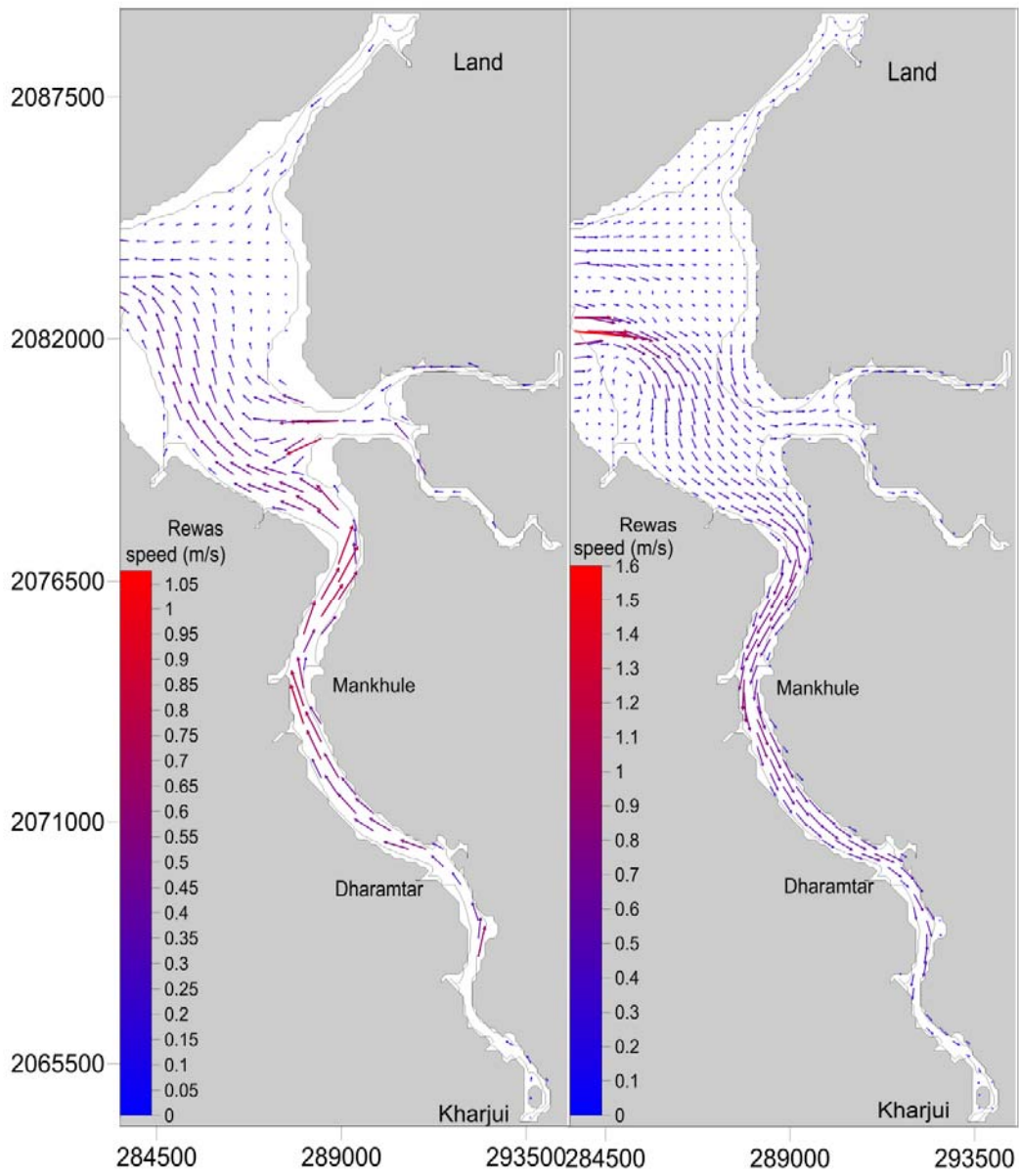


Figure 6

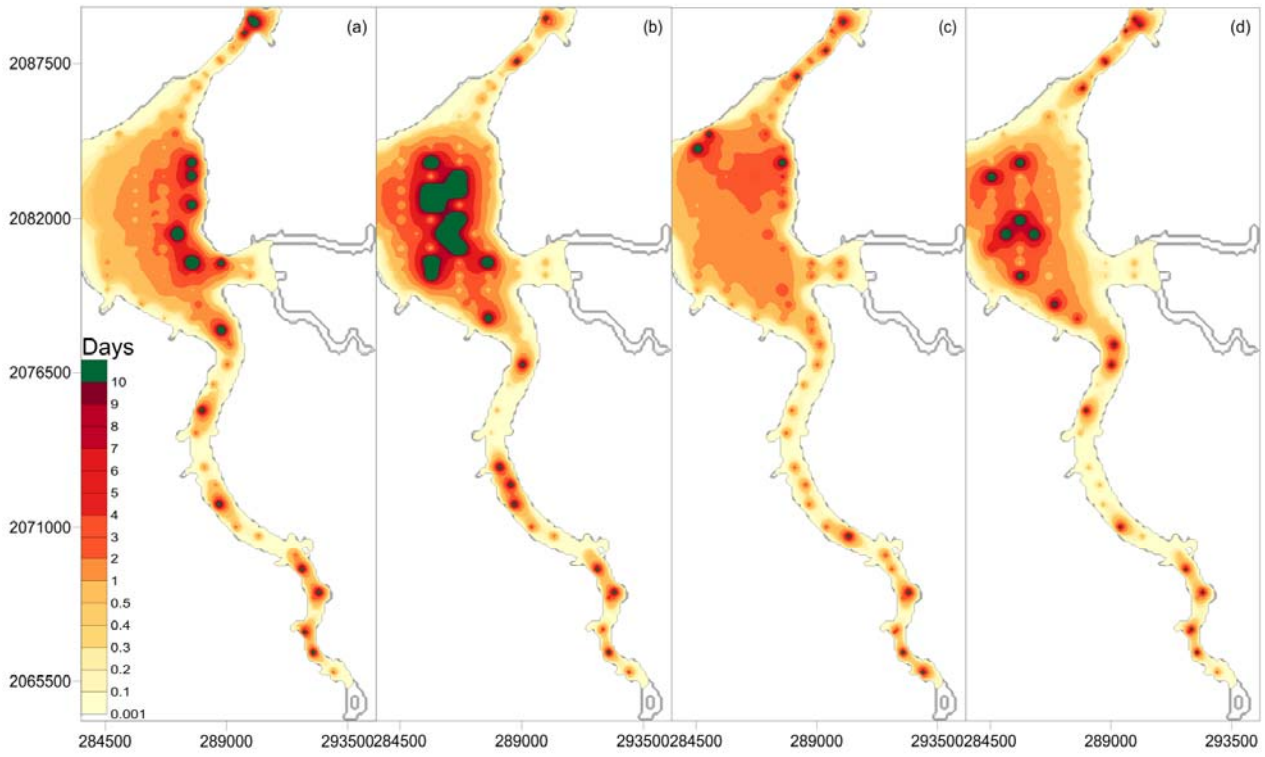


Figure 7

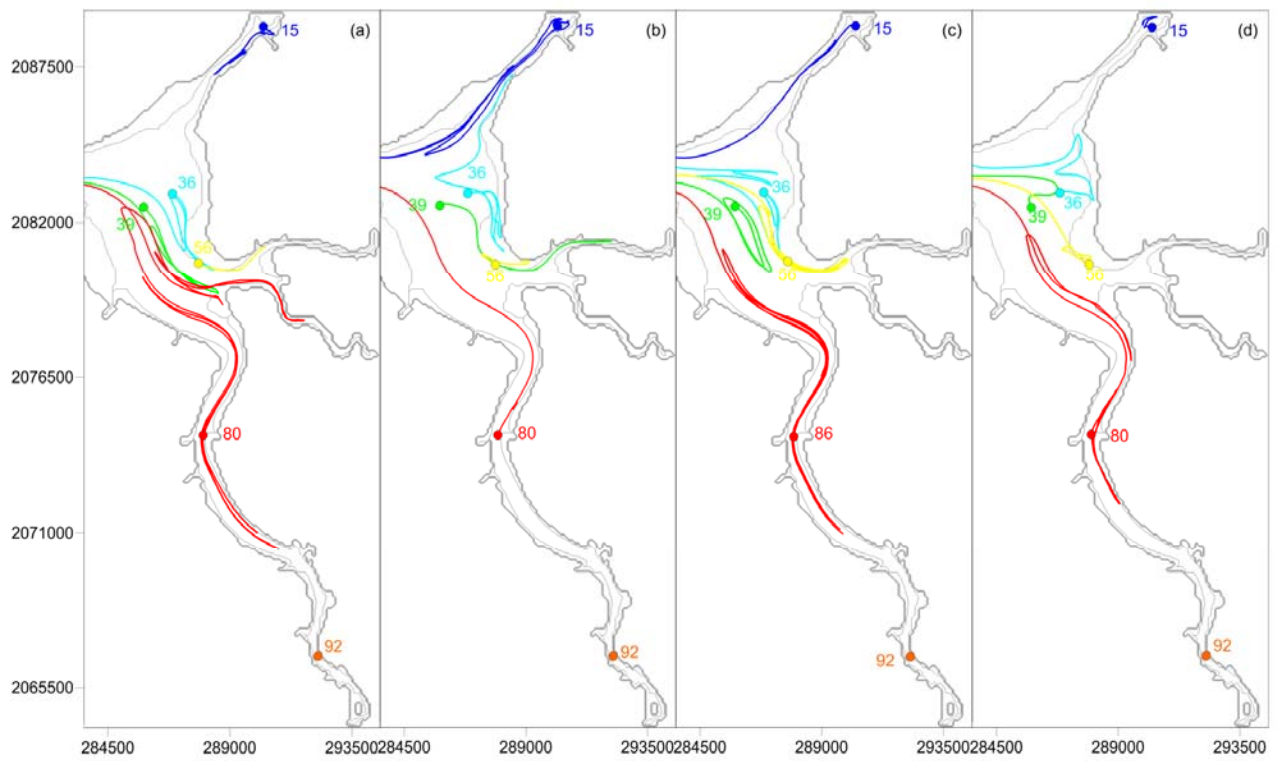


Figure 8

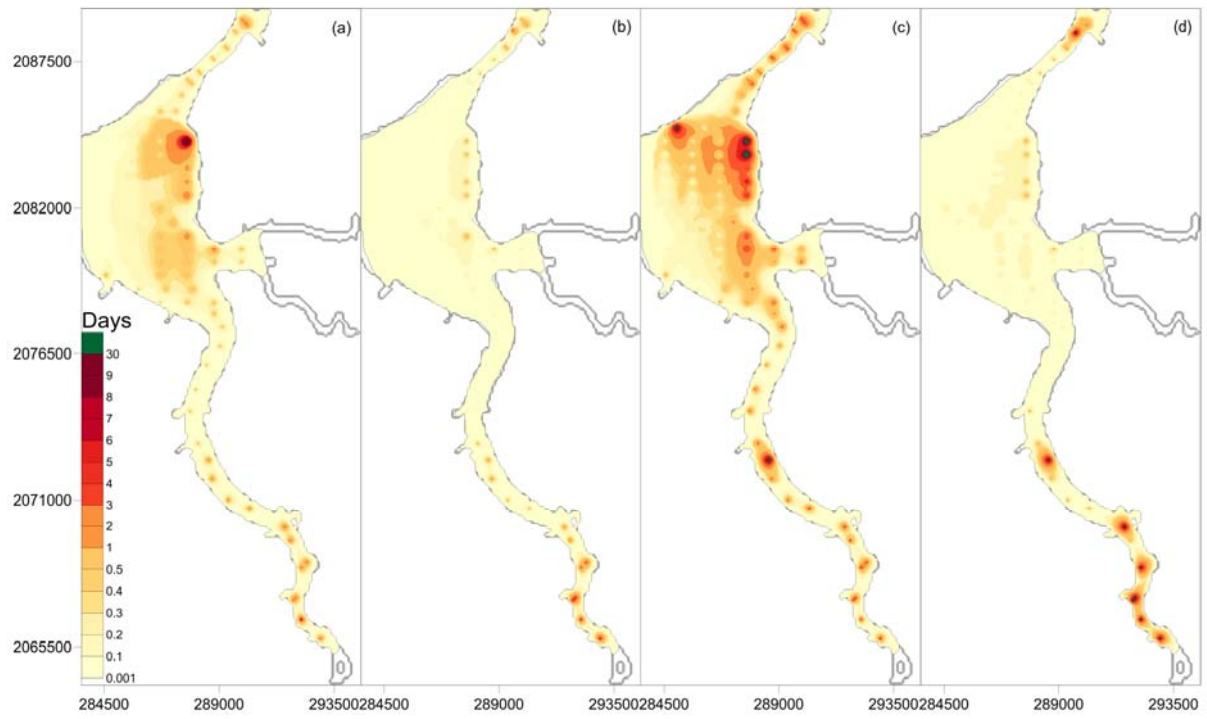


Figure 9

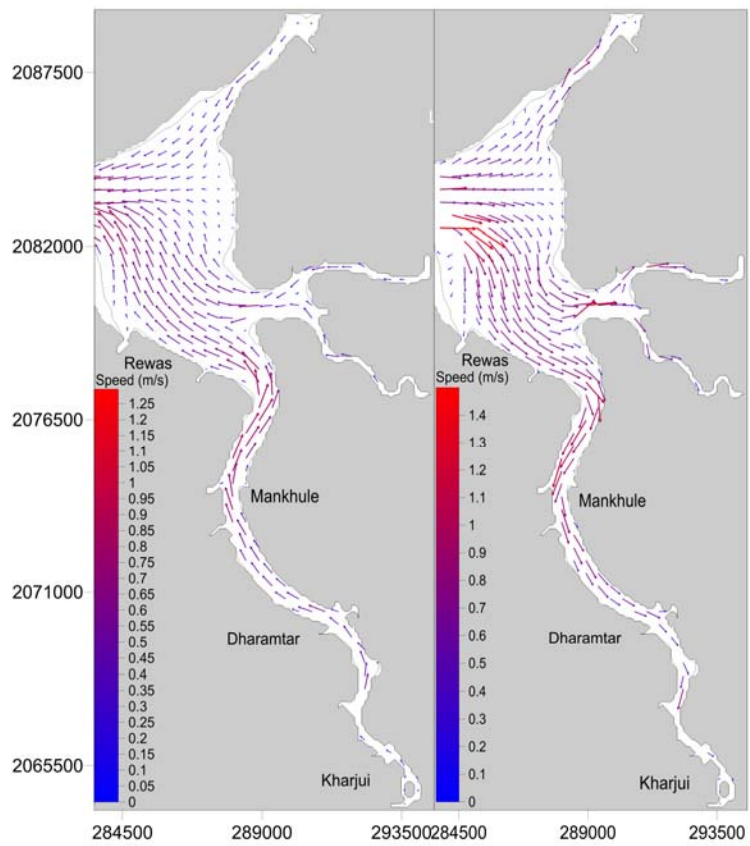


Figure 10

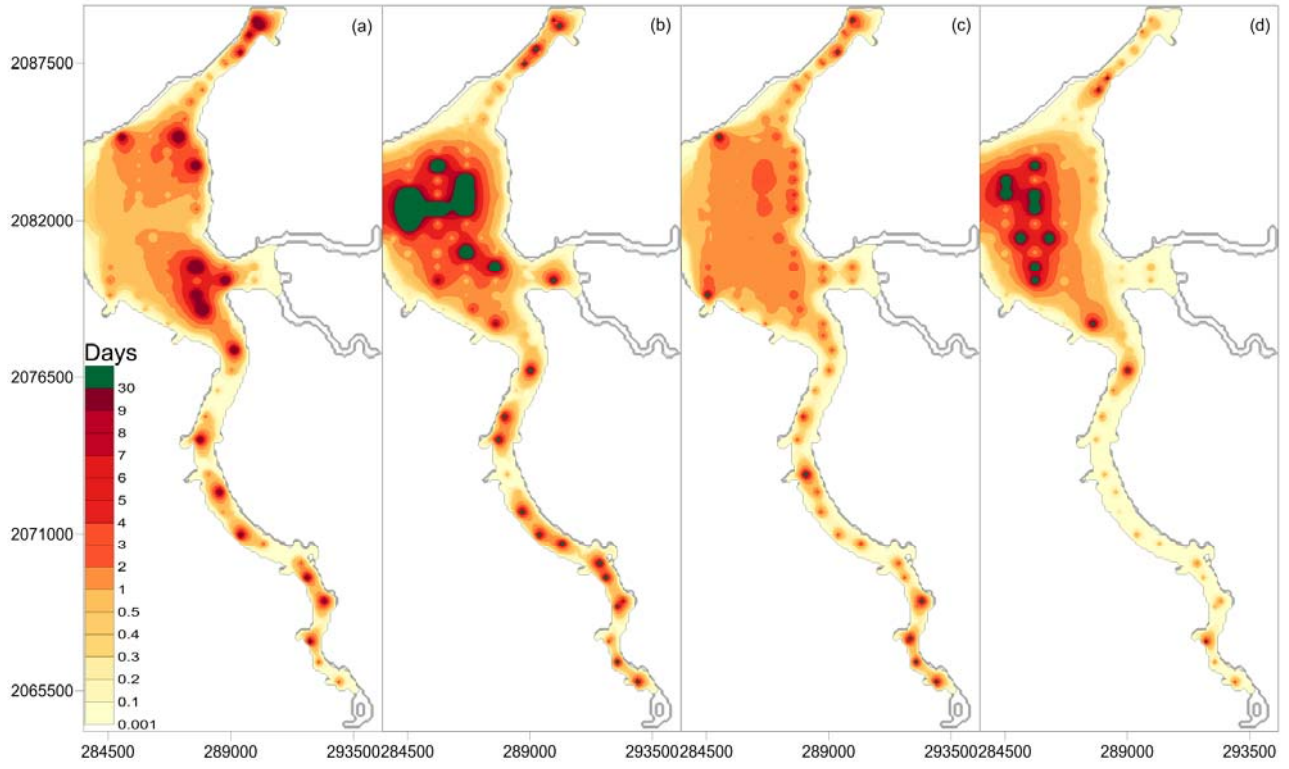


Figure 11

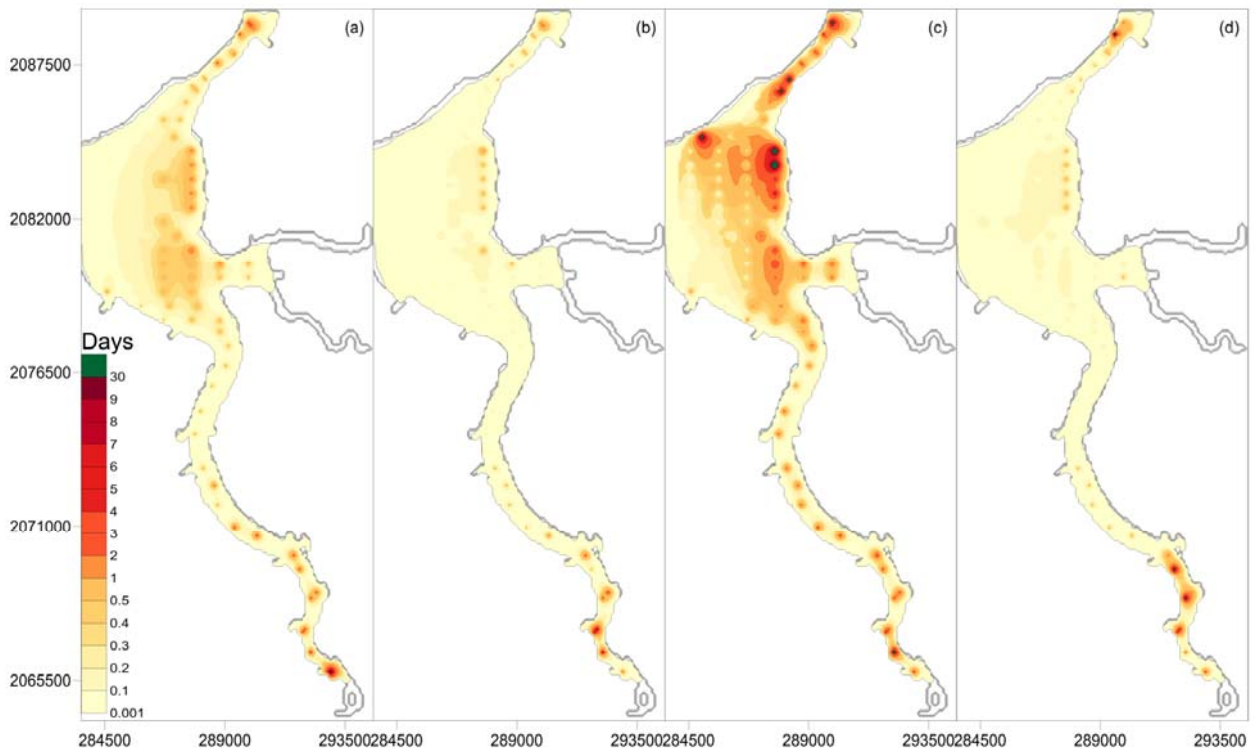


Figure 12

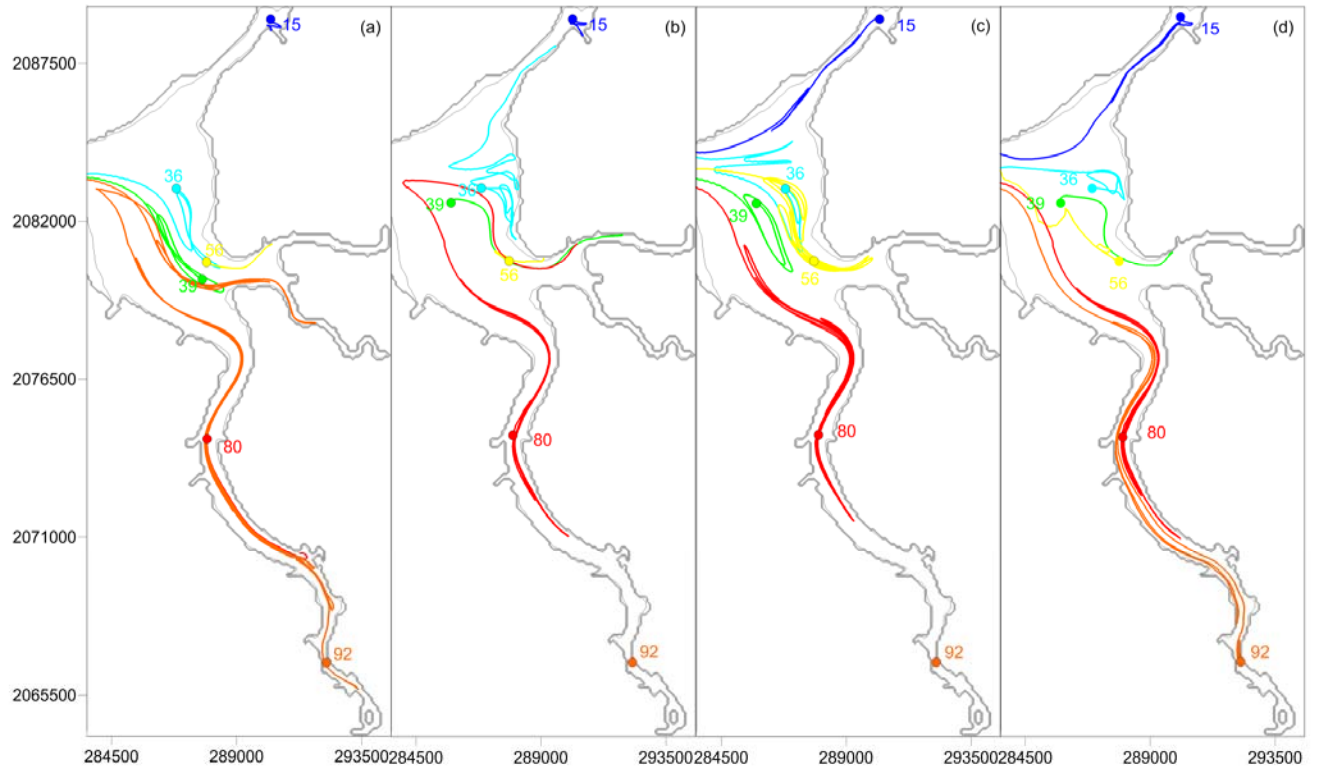


Figure 13

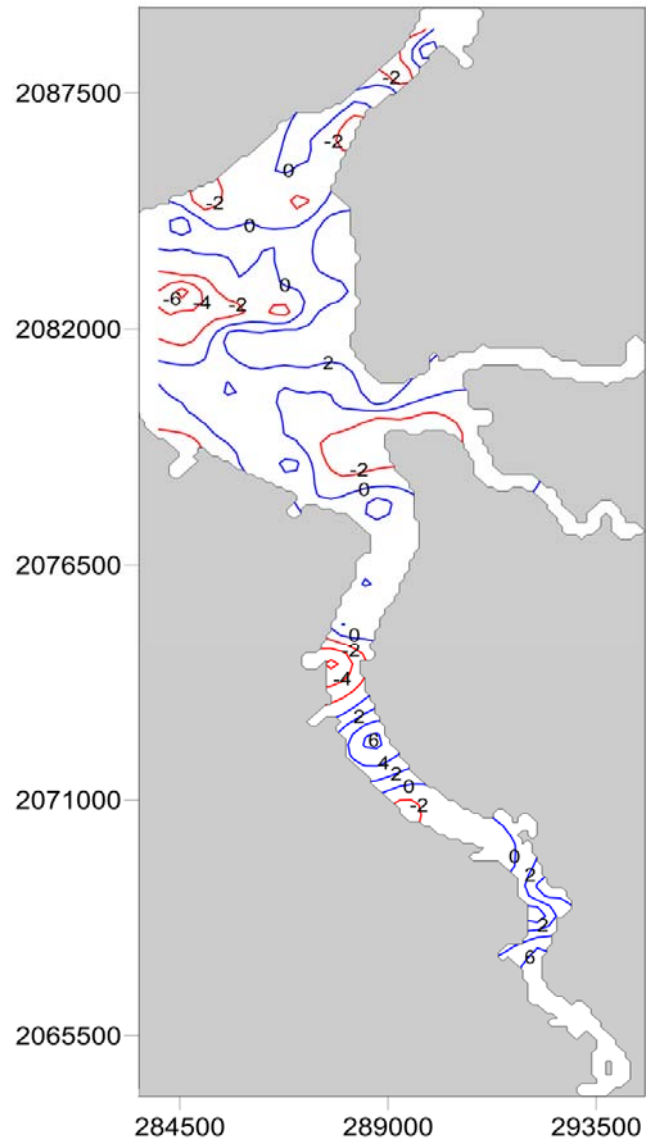


Figure 14